

Article citation info:

Castilla-Gutiérrez J, Fortes JC, Davila JM. Control and prediction protocol for bearing failure through spectral power density. *Eksplloatacja i Niezawodnosc – Maintenance and Reliability* 2020; 22 (4): 651–657, <http://dx.doi.org/10.17531/ein.2020.4.8>.

Control and prediction protocol for bearing failure through spectral power density

Indexed by:



Javier Castilla-Gutiérrez*, Juan Carlos Fortes, Jose Miguel Davila

Department of Mining, Mechanical, Energy and Construction Engineering, Higher Technical School of Engineering, University of Huelva, 21007 Huelva, Spain

Highlights

- Rotating elements are one of the main failure causes in production systems.
- Analysis of the SKF6322 bearing in real use conditions during 15 years.
- The analysis concluded that SPEED has been the most significant frequency.
- This study could help improve predictive maintenance by reducing monitoring times.

Abstract

This paper aims to analyse the results of the comparative study of the characteristic frequencies, in terms of Power Spectral Density (PSD), generated by an SKF6322 bearing in a rotational blower. Among all the analysed frequencies, we have focused on the ones generated by the shaft rotation speed, the one on the blades and the ones of the SKF6322 bearing, such as the tracks, the cage and the balls. For this study, we followed the ISO 10816 criteria, both in the sampling part and in the data analysis, using the speed values in terms of PSD, which improves the results in both high and low frequencies. This study can be used to predict the performance of bearings and their future failure, determining the most decisive frequency, the one with the highest incidence and the relative influence of each one on the different positions and monitoring coordinate axes. This procedure can be applied to improve the predictive maintenance protocol in order to improve the performance, efficiency and reliability of the equipment with bearings in their systems.

Keywords

vibration, bearing, diagnostics, vibroacoustics.

This is an open access article under the CC BY-NC-ND license (<http://creativecommons.org/licenses/by-nc-nd/4.0/>)

1. Introduction

Maintenance and reliability is a fundamental tool for production sites and companies in general, because they represent a competitive advantage. This is because it helps reducing the costs of time, material and, above all, production losses. Therefore, there is a great demand for improving preventive and especially predictive maintenance protocols [15], in terms of industrial equipment and among them the most sensitive element, which are bearings. [25]. About 40% of shutdowns are caused by bearings [23], which is why it is important to improve control and monitoring procedures.

Bearing failure depends on many variables, such as: assembly, preventive maintenance, lubrication control [30], excessive dynamic loads, fatigue [5], design faults, handling defects, impacts or contamination [14]. Common work methodology for bearing failure diagnosis and analysis follows the maximum amplitude value prescriptions, according to the international standard ISO10816, without addressing the effect of independent frequencies of each part of the equipment and each bearing. Each control point and each axis receives data on power density or RMS [2].

Following the ISO, speed is used as a sampling variable. So, in terms of power density, it does not use the energy generated from the frequency spectrum of the acceleration, which masks defects at low frequencies. Also not using the density produced by the dis-

placement that masks the high frequencies. Another problem with this technology is the requirement to measure frequently at all points to avoid the effect of bearing failure [29]. The 4 stages specified by the international standard ISO indicates the vibration levels supported by the machine. This wrong performance is caused by improper working conditions, eccentric misalignment, defective shafts and cavitation [19] and it is in the last stage when the bearing breaks down completely [26].

Early research addressed the problem by improving signal quality through measurement sensors and processing. The aim is to identify the stage of the bearing. In the first and second stage the defect is not perceptible, neither visually nor audibly using classical methods of vibration measurement and analysis. In the third stage, there is a small increase in temperature, but it is a challenge to monitor it. The transition from the third to the fourth phase is very fast due to the type of breakdown in the form of a ski curve, and it is in this last phase where the prediction has no value, since it implies predictive actions on the equipment [18]. Another factor for prediction is the number of equipment types and defects [20], because it is not only important to determine the stage, but also to know the most sensitive parts to the energy effect of this type of disturbances.

New non-invasive techniques such as acoustic studies are trying to improve predictive maintenance [12] but they have the problem of the working environment. These studies produce results in laboratories

(*) Corresponding author.

E-mail addresses: J. Castilla-Gutiérrez - javier.castilla@dimme.uhu.es, J.C. Fortes - jcfortes@dimme.uhu.es, J.M. Davila - jmdavila@dimme.uhu.es

but in the real field their results are not satisfactory. Currently, vibration techniques are the best answer to the problem, but the cost of this type of maintenance is very expensive due to the number of elements that interact [16]. The disadvantage of the vibration spectral study is that it requires a frequent control and monitoring of all the axes and positions to see the evolution and optimize the best time to make repairs or improvements [21]. Knowing the elements and control positions that are most sensitive to vibrations is a competitive advantage in the industrial sector, since it enables to predict failures. This results in great efforts to obtain them. Studies deal with the problem in laboratories with controlled conditions, analysing the effect of internal stress, dissipation or energy produced by roughness, without being able to evaluate the effect of real conditions [1], due to the time needed to perform this type of monitoring. Most studies approach the problem in laboratories [11]. The effect of internal stress, dissipation or energy produced by roughness is analysed, as well as new designs with gas application, to minimize the effects of tangential and centrifugal forces [4]. Other studies approach the problem by experimenting with Vectorial Support Machines (VSM) [8], looking for early diagnosis of ball bearing failure through Wavelet signal processing [6]. Most studies to date are conducted in laboratories and those conducted in the field have a smaller sample size. They also approach the problem in an isolated way, one defect at a time, and in controlled environments, without considering how each of them affects the maximum amplitude value, which is the reference value used for maintenance and reliability of industrial equipment [7].

Real monitoring measurement points are neither addressed, nor do they respond to real working conditions performance and always have the problem of limited sample number, using stochastic methods that are not subsequently validated in situ [28]. This paper therefore analyses the problem by monitoring a device under real working conditions. This study improves maintenance and reliability protocols by reducing the number of control points, which translates into time savings, improved efficiency, and an increase of the monthly number of samples. The analysis through the spectral value of each independent frequency allows to know the most sensitive element to breakage and its control point, this would help to make changes in the bearing design and engineering. Another added value of this research is that it has been conducted through a 15-year sampling under real working conditions, which have validated this maintenance method.

2. Material and methods

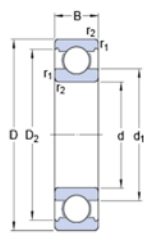
2.1. Equipment under study

We analyse the vibration of the bearing SKF6322 in equipment with the following specifications: frame size 400 motor weighing 3190 kg, with a wingspan of 1900 x 910 mm, steel bedplate of 2100 x 3900 x 300 mm. The powered equipment has a 2075 mm. diameter fan; and a 95 mm and 3900 mm long shaft. The driven equipment has a 2075 mm. diameter fan; a 95 mm. and 3900 mm. long shaft. The blades are powered with a coupler, the motor part is 1900 mm long and the fan is 2000 mm long.

The fault frequency of the different parts in the bearing is defined according to the contact points [13]. This bearing generates 5 characteristic frequencies, which would be the BSF or ball spin frequency or the rollers; the FTF (Fundamental Train Frequency) or the one generated by the cage, the incidence on the inner or outer track called ball-pass inner race (BPIR) and ball-pass outer race (BPOR) respectively. Another very important variable is that generated by the second harmonic of the balls, which is usually a more accurate indicator than their fundamental harmonic [31].

The equipment under study has as fundamental bearing the SKF6322, which supports the part of the blades. Table 1 shows the nominal specifications of this bearing.

Table 1. SKF6322 bearing specifications

Basic dynamic load (C)	C 203 kN	
Basic static load (C0)	C0 180 kN	
Fatigue limit load (Pu)	Pu 5.7 kN	
Reference speed	6000 r/min	
Speed limit	5300 r/min	
Calculation factor (kr)	kr 0.03	
Geometric characteristics	d = 110 mm D = 240 mm B = 50 mm d ₁ ≈ 149.5 mm D ₂ ≈ 207 mm r _{1,2} = 3 mm	

In addition to the previously described variables related to the bearing, we will also analyse those generated by the rotation of the machine itself (SPEED) and those caused by the rotation of the blades. For data collection, we have followed the indications of the ISO

Table 2. Characteristic frequencies of the SKF6322 bearing (Hz)

Frequencies	FAGNU322
FTF	568.58
BSF	2986
2BSF	5971.9
BPOR	4550.5
BPIR	7366.6
Speed	1490
Blades Fpa	13410

10816.3 standard [32]. The bearing, blower shaft and blade frequencies are shown in Table 2.

The analysis of the frequency of rotation of the equipment and the blades is an indispensable requirement to be able to validate the energy weight generated by each one and between them, and with future studies it would be possible to determine or to see the affection of these variables with other operation regimes.

2.2. Vibration analysis

The predictive analysis of a rotating machine comes from the transformation of the signals caused by the vibrations generated by this equipment. Fourier succeeded in relating the shape of the waves generated by vibrations to the frequency, generating their vibratory spectrum [17]:

$$X(f) = \int_{-\infty}^{\infty} x(t) * e^{-j2\pi ft} dt \quad (1)$$

The representation of the frequency spectrum is called spectral density, which is achieved by decomposing the waves generated by the vibrations represented as a function of frequency rather than time. The analysis of failure detection by means of signals in the frequency domain does not allow a guaranteed approach. Therefore, there arises the concept of Power Spectral Density (PSD) which is the amount of energy that each characteristic frequency has, and which follows the following mathematical equation:

$$PSD(x(i)) = \frac{1}{T} \sum (x(i))^2 \Delta T \quad (2)$$

The sum x (i) for ΔT is the average power of the range or the sum of the powers of the different components, independently. To estimate this energy, we limit the integration interval by using a rectangular window of the sample function. This window is defined as a periodogram and has the advantage of detecting hidden frequencies [9]. There are more accurate methods for analysis, one of them is the Hilbert

HT (Hilbert Transform) transform, which studies the signal envelope. This achieves an improved PSD and optimizes the sampling in vibrations that are generated at low frequency, modulating the primary signal [27]. The method follows the procedure of transforming two functions $s(t)$ and $1/(\pi)$ into a third one, as shown in mathematical expression number 3:

$$\bar{x}(t) = \frac{1}{\pi} \int_{-\infty}^{\infty} x(u) \frac{1}{t-u} du \quad (3)$$

This system amplifies the events that are generated at low frequency, by means of the components that form the signal's envelope. The system provides improvements, but also has its weaknesses, as it is very sensitive to noise [24]. This problem was solved using the Wavelet Transform (WT) [10]. This provides information on two study variables in signal processing, such as time and frequency [22].

3. Data acquisition, processing and analysis

For data collection and processing of vibrations, we have used the Entel IRD analyser and the Odyssey Emonitor software. The computer equipment has a 16-channel interface, a 4-filter multiplexer, with an integrator for the generation of velocity signals as a function of acceleration and similarly as a function of displacement. To avoid aliasing high frequencies, the received signal is amplified and filtered. Finally, the system has an analogue-digital converter, which captures up to 51.2 kHz, with a resolution of 16 bit.

The Odyssey Emonitor Software allows for the generation of trend graphs of vibration energy levels and their characteristic frequencies. The accelerometer used has a sensitivity level of 100 mV/g, with a contact displacement translator, which allows a frequency range of 10,000 Hz. We used a magnet anchorage method with quick release grip to secure it. This allows to reach failures in a higher frequency range, with a sensitivity range compressed between 0-300 Hz. Monitoring is carried out using a Hanning window of 3,200 to 60.000 spectral lines for vibration velocity and of 3,200 to 60,000 for acceleration, obtaining a bandwidth of 28 CPM and 140 CPM for speed and acceleration, respectively. The resolution obtained will be 18 CPM and 93 CPM for speed and acceleration, respectively. The standard used for diagnosis has been ISO10816. The equipment consists of two control and data acquisition points identified with numbers 3 and 4; at each of these points, data is collected according to the three coordinates of space X, Y, Z. The digital integration weighs up the signals produced at low frequencies, acting to a lesser extent on the high ones. This is because the speed $V(f)$ is inversely proportional to the frequency f . as can be seen in the following expression:

$$V(f) = \frac{c_1 A(f)}{f} \quad (4)$$

While the $D(f)$ shift is equally affected by frequency, but in an exponential manner:

$$D(f) = \frac{c_2 A(f)}{f^2} \quad (5)$$

where $A(f)$ is the acceleration at frequency f and C_1 and C_2 are constants depending on the measurement units.

Following the indications of the previously mentioned standard, the maximum levels in terms of RMS are used, where a total of 617 shots are obtained for each of the two positions and the three coordinated axes, resulting in a total of 3702 data.

4. Results and discussion

Initially, we study which part of the bearing has the greatest impact on the equipment's operation, in terms of RMS speed. To do this, the maximum amplitude values are taken and compared with each average position separately, comparing the incidence on each axis.

After determining the axis of each most incident position, it will be compared with that of the other position, to determine which of the two is the most sensitive to the energy effect of vibration. Once each frequency's position and axis have been determined, the most harmful frequency will be evaluated in order to study how it behaves with the equipment's operating frequency, called SPEED, and the frequency of the blades. We start with the analysis of the frequency generated by the bearing cage, calculating the sum of values obtained throughout the study in each position and its axes. We do the same with the mean and the maximum or peak value, all in terms of RMS. In table 3 the result is evaluated first by positions, where position four has a higher energy value than position three, this means that the FTF has a greater impact on it. Another value to be noted is the performance of the axes. The vertical axis is the one that obtains a higher RMS value at both mean points. This indicates that the disturbances generated by the ball cage are more incident on this axis (table 3).

Table 3. FTF results in terms of RMS (mm/s)

VARIABLE	POS3H	POS3V	POS3A	POS4H	POS4V	POS4A
TOTAL SUM	86,207	112,649	45,723	195,297	218,639	64,424
AVERAGE	0,141	0,184	0,075	0,319	0,357	0,120
PEAK VALUE	2,454	5,870	0,744	7,457	9,463	1,341

As a conclusion, it must be said that the highest values correspond to the vertical axes and specifically the one in position 4 is higher, both in general terms and in peak values. But to determine the viability of the method, the results are checked over the whole sample period. In graph number 1 the results of the variable FTF can be checked, in positions 3 and 4 vertical.

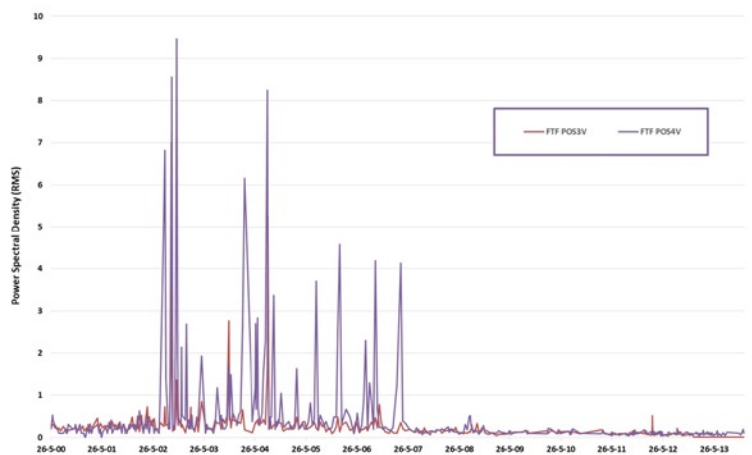


Fig. 1. FTF results in terms of RMS (mm/s) in positions 3 and 4 vertical

Apart from the values, the most important thing is to detect that this variable follows a common pattern in both positions, only varying the peak and the absolute values. Another factor is the homogeneity of both, following a common pattern, which is a fundamental fact to be able to state that it would only be necessary to sample the vertical position 4 for an early failure detection, avoiding the sampling of 5 more positions.

After evaluating the frequency of the bearing cage, we continue with the analysis of the effect caused by the frequency of the balls. When analysing the results, the result obtained in FTF is repeated:

position 4 is the most decisive, with an average value of twice the one obtained in position 3. The sampling by incidence axis, shows that the vertical axis is more important. It should be noted that in the case of checkpoint 3, the results are very similar, so it can be said that this frequency is affected by position 4 and, unlike FTF, it becomes homogeneous. This is shown in table 4.

The highest values are found to correspond to the vertical axis of position 4, followed by the horizontal position 3. The whole evolution of the sampling period is shown in graph 2. As in the previous case, this variable follows a common pattern in both positions, even if they have different axes, only varying the peak and absolute values. It is important to say that in absolute values, FTF reaches peak values 10 times higher than BSF, and in the case of accumulated values for the whole sample, the latter do not even reach a quarter of those obtained in FTF. Afterwards, we evaluate the effect caused by the impact frequency of the balls on the outer track. It is observed that position 3 is the most

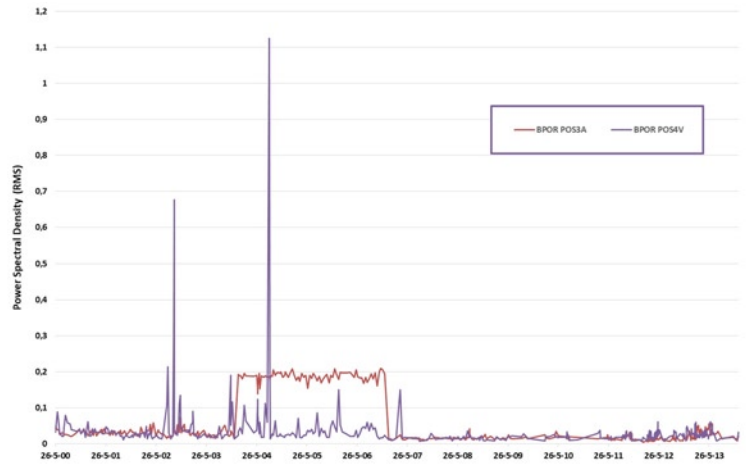


Fig. 3. BPOR results in terms of RMS (mm/s) at positions 3 axial and 4 vertical

Table 4. BSF results in terms of RMS (mm/s)

VARIABLE	POS3H	POS3V	POS3A	POS4H	POS4V	POS4A
TOTAL SUM	17,378	18,013	26,207	14,980	18,351	13,763
AVERAGE	0,028	0,029	0,043	0,024	0,030	0,026
PEAK VALUE	0,253	0,358	0,209	0,240	1,125	0,130

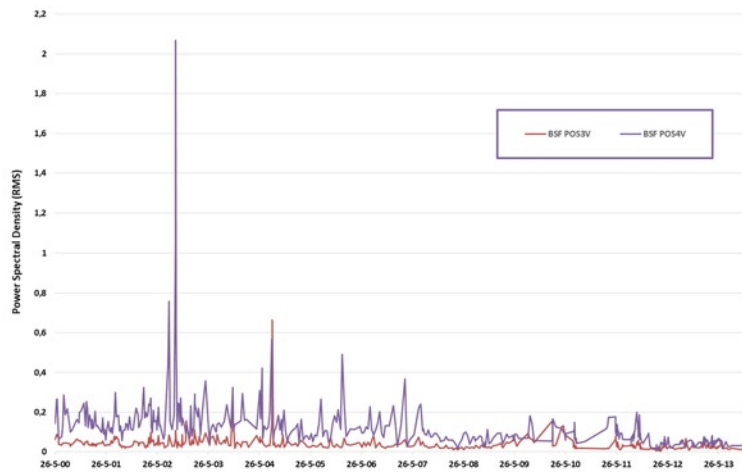


Fig. 2. BSF results in terms of RMS (mm/s) in positions 3 and 4, vertical

Table 5. BSF results in terms of RMS (mm/s)

VARIABLE	POS3H	POS3V	POS3A	POS4H	POS4V	POS4A
TOTAL SUM	14,427	15,081	8,836	15,466	15,974	7,963
AVERAGE	0,024	0,025	0,014	0,025	0,026	0,015
PEAK VALUE	0,169	0,160	0,068	0,291	0,465	0,058

Table 6. BPIR results in terms of RMS (mm/s)

VARIABLE	POS3H	POS3V	POS3A	POS4H	POS4V	POS4A
TOTAL SUM	14,427	15,081	8,836	15,466	15,974	7,963
AVERAGE	0,024	0,025	0,014	0,025	0,026	0,015
PEAK VALUE	0,169	0,160	0,068	0,291	0,465	0,058

Table 7. 2BSF results in terms of RMS (mm/s)

VARIABLE	POS3H	POS3V	POS3A	POS4H	POS4V	POS4A
TOTAL SUM	14,427	15,081	8,836	15,466	15,974	7,963
AVERAGE	0,024	0,025	0,014	0,025	0,026	0,015
PEAK VALUE	0,169	0,160	0,068	0,291	0,465	0,058

determining, breaking thus the results of the FTF and BSF frequencies. The previous sequences are also broken in the axes, having the highest mean and peak value in POS3A. Everything previously stated indicates that the vibration generated on the outer track causes more disturbances on the axial axis of position three, followed by the vertical axis of position 4. The maximum and accumulated energy values of the BPOR variable are shown below in table 5. The highest values correspond to the axial axis of position 3, followed by the vertical position 4. To determine if they follow a common pattern and how the evolution of the maximum peaks has been, we conduct a comparative representation, which will determine if the control method of fewer positions and measurement axes is valid for the successful predictive maintenance of this type of equipment. Results are shown in graph number 3. The graph shows homogeneity of results, where common patterns are obtained with periods of higher values in the axial position 3, as the period between 2004 and 2006, but its trace is homogeneous to the one generated in the vertical position 4.

Subsequently, we evaluate the effect caused by the impact frequency of the balls on the inner track or BPIR. This is shown in Fig. 3. The result is that the vertical position 4 is the most significant. It is important to mention the parity between the horizontal and vertical axes. In the case of position 3 we obtain the value POS3V as the most sensitive. It is necessary to emphasize the equality of results by axis, taking as second important axis the horizontal one. The values obtained in POS4V are very similar to those obtained in POS3V, which indicates that this variable generates a similar effect whatever its control point is, allowing it to be monitored in both positions without any discrimination in the results (table 6). The following step is to verify the evolution in the whole sampling period, see fig. 4: As in the previous case, the variable BPIR follows a common pattern in both positions and axes, varying only the peak and absolute values. Obtaining common patterns indicates that checkpoint and sampling decrease is a reality to control this variable, with the consequent savings in terms of time and material.

After evaluating the BPIR frequency of the bearing, we assess the effect caused by the second harmonic of the balls, because sometimes higher values can be obtained for this variable, in the second harmonic. This time, the results compared to BSF are lower, both in cumulative values and in peak values, we can also see a uniformity in cumulative values. The analysis determines that position 4 remains the most influential one in relation to the measurement axis and the vertical axes the most sensitive to the effect of this vibration. The analysis of 2BSF can be seen in table 7. The highest values correspond to the vertical axis of position 4, followed by horizontal position 3.

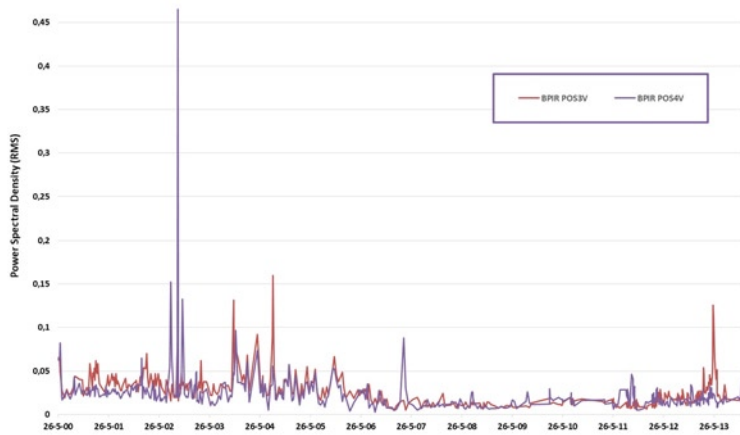


Fig. 4. BPIR result in terms of RMS (mm/s) at positions 3 vertical and 4 vertical

Table 8. Results of all bearing frequencies in terms of RMS (mm/s)

VARIABLE	POS3H	POS3V	POS3A	POS4H	POS4V	POS4A
TOTAL SUM	14,216	20,815	10,048	18,414	20,940	9,039
AVERAGE	0,023	0,034	0,016	0,030	0,034	0,017
PEAK VALUE	0,112	0,170	0,079	0,382	0,614	0,066

Table 9. Results of all bearing frequencies in terms of RMS (mm/s)

VARIABLE	SPEED POS4V	FTF POS4V	ALABES POS3A
TOTAL SUM	14,216	20,815	10,048
AVERAGE	0,023	0,034	0,016
PEAK VALUE	0,112	0,170	0,079

The evolution throughout the sampling period is shown in figure 5. As in the preceding case, this variable follows a common pattern in both positions, varying only the accumulated peak and average values.

After evaluating the bearing frequencies, its position and axes, the most determining variable is the one produced by FTF and its vertical position 4 is the most sensitive, see table 8. After determining the most significant bearing frequency, this is compared with the results of the other two study variables, SPEED and BLADES. Other studies have shown that these generate more incidence in the vertical positions 4. In the case of the machine and blades, this would be the axial position 3 [3]. Table 9 shows a comparison of the three. In the following graph the result of the three frequencies is shown and, with no linearity, the monitoring of the equipment is guaranteed through the two positions POS4V and POS3A.

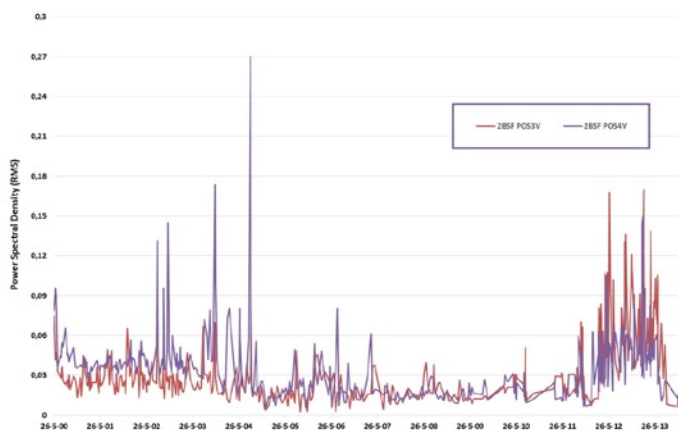


Fig. 5. Results of 2BSF in terms of RMS (mm/s) in positions 3 horizontal and 4 vertical

5. Conclusions

After analysing the most representative variables of the SKF6322 bearing, through the approximation method using power density values in RMS, we can conclude that the most important values are found in position 4, and the vertical axis is the most sensitive to the mechanical actions of the equipment.

If the variables are analysed separately, the frequencies generated by the ball cage, the balls themselves, the one generated in the inner track and the second ball harmonic have more incidence in vertical position 4. In the case of the frequency generated in the inner track, its action is greater in axial position 3.

In absolute and accumulated terms, the frequency generated by the cage obtains values four times higher than the frequency following it, which would be that generated by the bearing balls.

When comparing the FTF variable with the most important variables of the equipment, such as the equipment spin speed (SPEED) and blades (ALABES), it can be seen that, except for the blades, the other two are more incidental in the vertical position 4 and the action of the blades generates more disturbances in the axial position.

As a conclusion, it can be said that out of the 6 measurement positions and the 42 study variables, it is possible to predict the bearing and the equipment failure only by monitoring the vertical position 4 and the SPEED variable.

This allows to reduce by 83% this machine sampling and increase the number of monthly tests, improving prediction, reliability, maintenance, and production at the same cost.

Thanks to this study, the problem can be addressed at its roots, trying to reduce the effects of the rotational frequency and the acquisition of a better performing bearing in the ball cage.

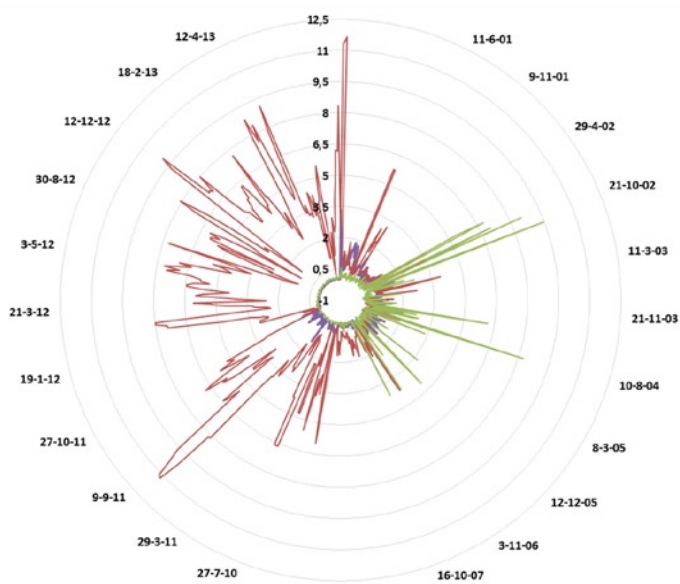


Fig. 6. Results of SPEED, FTF and Vane frequencies in terms of RMS (mm/s)

References

1. Artzer A, Moats M, Bender J. Removal of Antimony and Bismuth from Copper Electrorefining Electrolyte: Part I—A Review. *The Journal of The Minerals, Metals & Materials Society* 2018; 70: 2033–2040, <https://doi.org/10.1007/s11837-018-3075-x>.
2. Bo Sun, Mengmeng Li, Baopeng Liao, Xi Yang, Yitong Cao, Bofeng Cui, Qiang Feng, Yi Ren, Dezhen Yang. Time-Variant Reliability modeling based on hybrid non-probability method. *Archive of Applied Mechanics*, 2019, 90(2): 209-219, <https://doi.org/10.1007/s00419-019-01605-1>.
3. Castilla-Gutiérrez J, Fortes JC, Pulido-Calvo I. Analysis, evaluation and monitoring of the characteristic frequencies of pneumatic drive unit and its bearing through their corresponding frequency spectra and spectral density. *Eksplatacja i Niezawodność – Maintenance and Reliability* 2019; 21 (4): 585–591, <http://dx.doi.org/10.17531/ein.2019.4.7>.
4. Chaudhry V, Kailas S V. Elastic-Plastic Contact Conditions for Frictionally Constrained Bodies Under Cyclic Tangential Loadin. *Journal of Tribology* 2013; 136 (1), <https://doi.org/10.1115/1.4025600>.
5. Chudzik A, Warda B. Effect of radial internal clearance on the fatigue life of the radial cylindrical roller bearing. *Eksplatacja i Niezawodność – Maintenance and Reliability* 2019; 21 (2): 211–219, <http://dx.doi.org/10.17531/ein.2019.2.4>.
6. Cong F, Chen G, Dong G. Vibration model of rolling element bearings in a rotor-bearing system for fault diagnosis. *Journal of Sound and Vibration* 2013; 332 (8): 2081–2097, <https://doi.org/10.1016/j.jsv.2012.11.029>.
7. Ding X, He Q, Luo N. A fusion feature and its improvement based on locality preserving projections for rolling element bearing fault classification. *Journal of Sound and Vibration* 2015; 335: 367–383, <https://doi.org/10.1016/j.jsv.2014.09.026>.
8. Goyal D, Choudhary A, Pabla B.S. Support vector machines based non-contact fault diagnosis system for bearings. *Journal of Intelligent Manufacturing* 2019; 1572-8145, <https://doi.org/10.1007/s10845-019-01511-x>
9. Gowid S, Dixon R, Ghandi S. Characterisation of Major Fault Detection Features and Techniques for the Condition-Based Monitoring of High-speed Centrifugal Blowers. *International Journal of Acoustics and Vibration* 2016; 21 (2), <http://dx.doi.org/10.20855/ijav.2016.21.2410>.
10. Houpert L. An Enhanced Study of the Load–Displacement Relationships for Rolling Element Bearings. *Journal of Tribology* 2013; 136: 011105, <https://doi.org/10.1115/1.4025602>.
11. Huang L, Huang H, Liu Y. A Fault Diagnosis Approach for Rolling Bearing Based on Wavelet Packet Decomposition and GMM-HMM. *International Journal of Acoustics and Vibration* 2019; 24 (2), 199-209, <https://doi.org/10.20855/ijav.2019.24.21120>.
12. Ise T, Osaki M, Matsubara M, & Kawamura S. Vibration Reduction of Large Unbalanced Rotor supported by Externally Pressurized Gas Journal Bearings with Asymmetrically Arranged Gas Supply Holes (Verification of the Effectiveness of a Supply Gas Pressure Control System). *Journal of Tribology* 2019; 141 (3): 031701, <https://doi.org/10.1115/1.4041460>.
13. Kausschinger B, Schroeder S. Uncertainties in Heat Loss Models of Rolling Bearings of Machine Tools, *Procedia CIRP* 2016; 46: 107 – 110, <https://doi.org/10.1016/j.procir.2016.03.168>.
14. Li H, Fu L, Zheng H. Bearing fault diagnosis based on amplitude and phase map of Hermitian wavelet transform. *Journal of Mechanical Science and Technology* 2011; 25 (11): 2731–2740, <https://doi.org/10.1007/s12206-011-0717-0>.
15. Li Y, Billington S, Zhang C, Kurfess T, Danyluk S, & Liang S. Adaptive prognostics for rolling element bearing condition. *Mechanical Systems and Signal Processing* 1999; 13 (1), 103–113, <https://doi.org/10.1006/mssp.1998.0183>.
16. Louhichi R, Sallak M, and Pelletan J. A Maintenance Cost Optimization Approach: Application on a Mechanical Bearing System. *International Journal of Mechanical Engineering and Robotics Research* 2020; 9 (5): 658-664, <https://doi.org/10.18178/ijmerr.9.5.658-664>.
17. Madoliat R, Ghanati M F. Theoretical and Experimental Study of Spindle Ball Bearing Nonlinear Stiffness. *Journal of Mechanics* 2013; 29: 633-642, <https://doi.org/10.101017/jmech201348>.
18. Malla C, Panigrahi I. Review of Condition Monitoring of Rolling Element Bearing Using Vibration Analysis and Other Techniques *Journal of Vibration Engineering & Technologies* 2019; 7: 407–414, <https://doi.org/10.1007/s42417-019-00119-y>.
19. Medina S, Olver A V, Dini D. The Influence of Surface Topography on Energy Dissipation and Compliance in Tangentially Loaded Elastic Contacts. *Journal of Tribology* 2012; 134 (1), <https://doi.org/10.1115/1.4005641>.
20. Medrano-Hurtado Z Y, Medrano-Hurtado C, Pérez-Tello J, Gómez Sarduy M, Vera-Pérez N. Methodology of Fault Diagnosis on Bearings in a Synchronous Machine by Processing Vibro-Acoustic Signals Using Power Spectral Density Ingeniería. *Investigación y Tecnología* 2016; 17 (1): 73-85, <https://doi.org/10.1016/j.riit.2016.01.007>.
21. Nagi G, Alaa E, Jing P. Residual Life prediction sin the absence of prior degradation know ledge. *IEEE Trans. Reliab.* 2009; 58: 106–116, <https://doi.org/10.1109/TR.2008.2011659>.
22. Nandi S, Toliyat H A, Li X. Condition Monitoring and Fault Diagnosis of Electrical Motors—A Review. *IEEE Transactions on Energy Conversion* 2005; 20 (4): 719–729, <https://doi.org/10.1109/TEC.2005.847955>.
23. Omeregbee H O, Heyns P S. Fault Classification of Low-Speed Bearings Based on Support Vector Machine for Regression and Genetic Algorithms Using Acoustic Emission. *J. Vib. Eng. Technol* 2019; 7: 455–464, <https://doi.org/10.1007/s42417-019-00143-y>
24. Orhan S, Aktürk N, Celik V. Vibration monitoring for defect diagnosis of rolling element bearings as a predictive maintenance tool: Comprehensive case studies. *NDT & E International* 2006; 39 (4): 293-298, <https://doi.org/10.1016/j.ndteint.2005.08.008>
25. Pawlik P. Single-number statistical parameters in the assessment of the technical condition of machines operating under variable load. *Eksplatacja i Niezawodność – Maintenance and Reliability* 2019; 21 (1): 164-169, <http://ds.doi.org/10.17531/ein.2019.1.19>.
26. Polimac V, Polimac J. Assessment of present maintenance practices and future trends. *IEEE/PES Transmission and Distribution Conference and Exposition. Developing New Perspectives* 2001; 2: 891-894, <http://10.1109/TDC.2001.971357>
27. Schnabel S, Marklund P, Larsson R, Golling S. The Detection of Plastic Deformation in Rolling Element Bearings by Acoustic Emission. *Tribology International* 2017; 110: 209-201, <https://doi.org/10.1016/j.triboint.2017.02.021>.
28. Toledo E, Pinhas I, Aravot D, Akselrod S. Bispectrum and bicoherence for the investigation of very high frequency peaks in heart rate variability. *Proceedings of the IEEE, Computers in Cardiology* 2001; 28: 667-670, <https://doi.org/10.1109/CIC.2001.977744>.
29. Wang J, Liang Y, Zheng Y, Gao, Zhang F. An integrated fault diagnosis and prognosis approach for predictive maintenance of wind turbine bearing with limited samples. *Renewable Energy* 2020; 145: 642-650, <https://doi.org/10.1016/j.renene.2019.06.103>
30. Wang N F, Jiangl D X, Yang W G Dual-Tree Complex Wavelet Transform and SVD-Based Acceleration Signals Denoising and its Application in Fault Features Enhancement for Wind Turbine. *Journal of Vibration Engineering & Technologies* 2019; 7: 311–320, <https://doi.org/10.1007/s42417-019-00126-z>.

- 31 Zheng D, Chen W. Thermal performances on angular contact ball bearing of high- speed spindle considering structural constraints under oil-air lubrication. *Tribology International* 2017; 109: 593–601 9, <https://doi.org/10.1016/j.triboint.2017.01.035>.
- 32 Zhou W, Habetler T G, Harley R G. Bearing Condition Monitoring Methods for Electric Machines: A General Review. *IEEE International Symposium on Diagnostics for Electric Machines, Power Electronics and Drives* 2007; 3-6, <https://doi.org/10.1109/demped.2007.4393062>.
- 33 Zuber N, Bajric R. Application of artificial neural networks and principal component analysis on vibration signals for automated fault classification of roller element bearings. *Eksploatacja i Niezawodnosc – Maintenance and Reliability* 2016; 18 (2): 299–306, <http://dx.doi.org/10.17531/ein.2016.2.19>.